Supporting Information for

A Three-Dimensional Vertically Aligned Functionalized Multilayer Graphene Architecture - An Approach for Graphene-based Thermal Interfacial Materials

Qizhen Liang,[†] *Xuxia Yao,*[†] *Wei Wang,*[†] *Yan Liu*[†] *and Ching Ping Wong*[†, ‡, *]

[†]School of Materials Science and Engineering, Georgia Institute of Technology, 771 Ferst Drive, Atlanta, GA 30332 USA. [‡]College of Engineering, the Chinese University of Hong Kong, Hong Kong. Email: cp.wong@mse.gatech.edu

S1- An AFM height image of A-fMGs surface and corresponding thickness information.

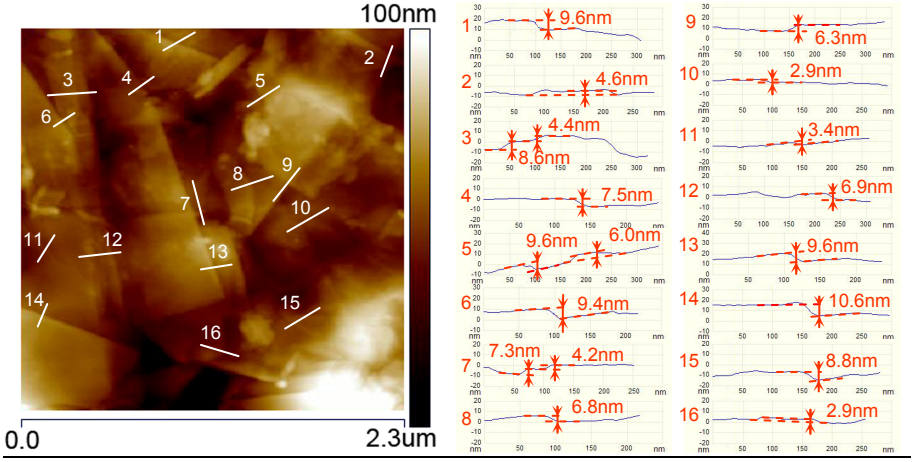

Figure S1. An AFM height image of A-fMGs surface and corresponding thickness information.

S2- Raman Characterization of functionalized multilayer graphene sheets (fMGs)

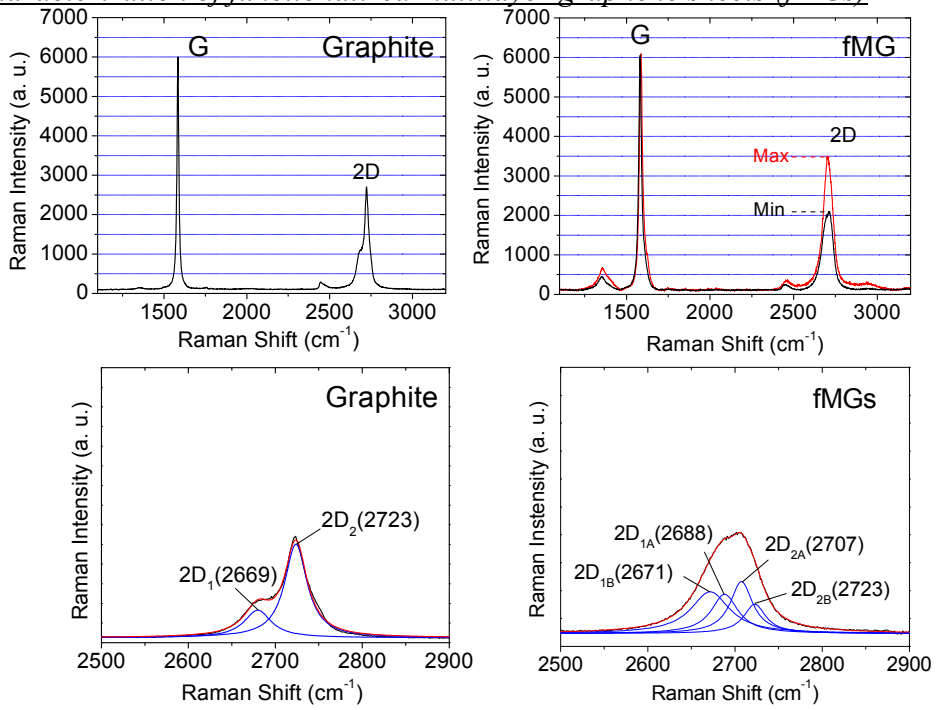

Figure S2. A comparison of Raman spectra between graphite and fMGs.

Electrical structure of graphene may influenced by defects and functional groups, e.g. carboxyls. Previous research reported by Eda *et al* (ref. 27 in main text) indicated that graphene oxide with oxygen-containing functional groups and a high defect level, has a board 2D peak with much lower intensity. Here, Raman spectrum of fMGs in Figure S2 shows 2D peak at ~2701±6 cm^{-1} with an intensity ranging from 1/3 ("Min" in Figure S2) to half ("Max" in Figure S2) of G band peak intensity. In contrast to an asymmetric 2D peak of graphite at ~2723 cm^{-1}, 2D peak of fMGs is symmetric. Further analysis also indicates that 2D peak in a typical Raman spectrum of fMGs can be corresponded to four peaks such as $2D_{1B}$ (~2671cm^{-1}), $2D_{1A}$ (~2688cm^{-1}), $2D_{2A}$ (~2707cm^{-1}), and $2D_{2B}$ (~2723cm^{-1}).

S3- A comparison of X-ray photoelectronics spectra between pristine graphite and fMGs.

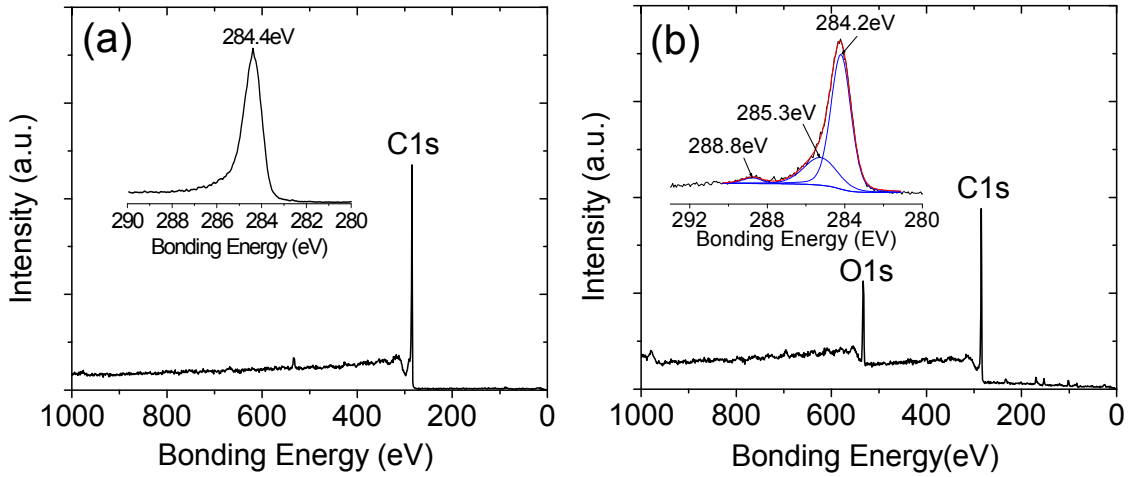

Figure S3. A comparison of XPS spectra between a) pristine graphite and b) fMGs. Inserted are related high resolution C1s spectra. The XPS spectra of fMGs shown here are identical with that of surface A in Figure 5 d and e.

According to Wagner *et al*'s work (ref. 42 in main text), the empirical atomic sensitivity factors for O1s and C1s are 0.66 and 0.25, respectively. Here, an empirical equation is applied in calculating concentration of oxygen on pristine graphite, side-wall surface (surface A) and cross-section surface (surface B) of A-fMGs.

$$C_O = \frac{\frac{P_O}{S_O}}{\frac{P_O}{S_O}+\frac{P_C}{S_C}} = \frac{\frac{P_O}{P_C}\frac{S_C}{S_O}}{\frac{P_O}{P_C}\frac{S_C}{S_O}+1}$$

Where C_O, P_O, P_C, S_O, and S_C present concentration of O atoms, integrated peak area of O1s from XPS spectrum, integrated peak area of C1s from XPS spectrum, atomic sensitivity factors for O1s, atomic sensitivity factors for C1s, respectively. Thus calculated concentrations of O atoms for prinstine graphite, sidewall of A-fMGs (surface A) and cross-section surface of A-fMGs (surface B) are ~2.5%, 17.7% and 33.8%, respectively, as listed in Table S1.

Table S1. A data list of oxygen concentration calculation based on low resolution XPS.

Sample	$\frac{P_O}{P_C}$	$C_O(\%)$
Prinstine graphite	0.069	2.5
A-fMGs (surface A)	0.571	17.7
A-fMGs (surface B)	1.347	33.8

S4- FTIR spectrum of fMGs.

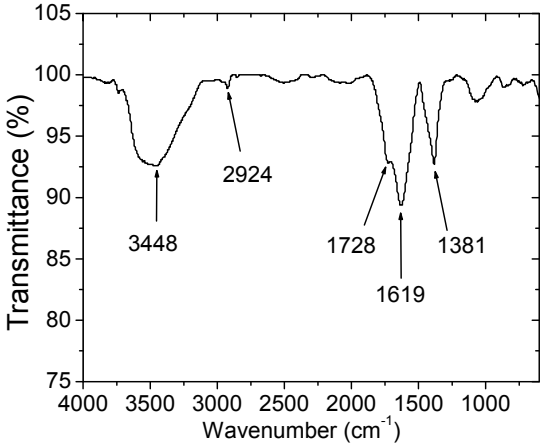

Figure S4. FTIR spectrum of fMGs shows peaks at 3448 cm^{-1} (-OH), 1381 and 1727 cm^{-1} (C=O).

S5- Thermal conductivity measurement of assembled A-fMGs TIMs

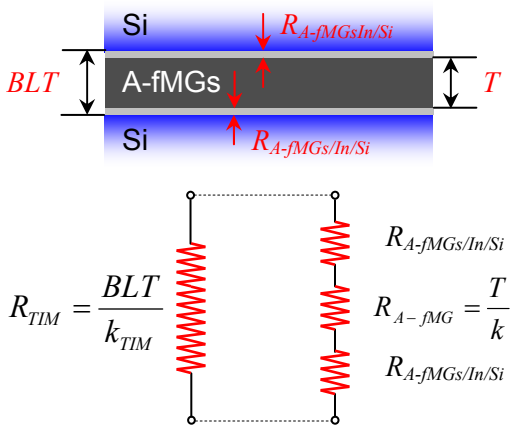

Figure S5. A schematic illustration of thermal conductivity measurement of assembled A-fMGs TIMs.

A light flash apparatus (LFA 447 NanoFlash, Netzsch Thermal Analysis) and a sophisticated analysis software (Proteus LFA Analysis, Netzsch Thermal Analysis) with a mathematical model designed for triple layer sandwich samples are applied in measuring equivalent thermal diffusivities of A-fMG TIMs (α_{TIM}) by experimentally collecting and mathematically fitting non-linear regression of data signal with consideration of heat loss. Here, as shown in Figure S5, measured α_{TIM} includes effects of interfacical thermal resistance across A-fMGs/In/Si interface ($R_{A\text{-}fMGs/In/Si}$) and intrinsic thermal resistance of A-fMGs. Two configurations of A-fMGs in TIMs layer are measured and compared. In one of the

configurations, an A-fMG sample is recumbent between Si surfaces. Bond line thickness (*BLT*) of the sandwiched recumbent A-fMG TIMs is 0.71 mm. In contrast, in the other configurations, A-fMGs are sliced and vertically stacked between Si wafers with a *BLT* of 2.3mm. As shown in Table S2, measured equivalent thermal conductivity (k_{TIM}, calculated from $k_{TIM} = \alpha_{TIM}\rho_{TIM}C_{p,TIM}$) of the described recumbent A-fMG TIMs (RA-fMG TIMs) and vertically stacked A-fMG TIMs (VA-fMG TIMs) are 1.39 and 75.5 W m^{-1} K^{-1}, respectively. Thermal resistance ($R_{TIM,}$ calculated from an equation of $R_{TIM} = \frac{BLT}{k_{TIM}} = 2R_{A-fMGs/In/Si} + \frac{T}{k}$) of the RA-fMG TIMs and VA-fMG TIMs are 511 and 30.5 mm^2 K W^{-1}, respectively, in which the contributions of intrinsic thermal resistance of A-fMGs count 426 and 20.3 mm^2 K W^{-1}. Thermal resistance across RA-fMGs/In/Si interface and VA-fMGs/In/Si interface is 42.5 and 5.1 mm^2 K W^{-1}, respectively. Uncertainty of $R_{A\text{-}fMGs/In/Si}$ shown in Figure 5b is valued according to an error transfer function as follows.

$$\delta R_{A-fMG/In/Si} = \frac{1}{2}\sqrt{\left(\frac{L\delta k_{TIM}}{k_{TIM}^2}\right)^2 + \left(\frac{T\delta k}{k^2}\right)^2}$$

where $\delta R_{A-fMGs/In/Si}$, δk_{TIM}, δk_{A-fMGs} are uncertainties of $R_{A\text{-}fMGs/In/Si}$, k_{TIM}, and k, respectively.

Table S2. A data list of thermal measurement of assembled A-fMGs TIMs.

Configuration	VA-fMG TIMs	RA-fMG TIMs
BLT (mm)	2.30	0.71
T(mm)	2.28	0.69
$\rho_{A\text{-}fMGs}$ ($g\ cm^{-3}$)	1.6	1.6
$C_{p,\ A\text{-}fMGs}$ ($J\ g^{-1}K^{-1}$)	0.73	0.73
$\alpha_{A\text{-}fMGs}$ ($mm^2\ s^{-1}$)	96.1	1.38
k [a] ($W\ m^{-1}\ K^{-1}$)	112.2	1.62
$R_{A\text{-}fMGs}$ [b] ($mm^2\ K\ W^{-1}$)	20.3	426
α_{TIM} ($mm^2\ s^{-1}$)	64.6	1.19
ρ_{TIM} ($g\ cm^{-3}$)	1.6	1.6
$C_{p,\ TIM}$ ($J\ g^{-1}K^{-1}$)	0.73	0.73
k_{TIM} [a] ($W\ m^{-1}\ K^{-1}$)	75.5	1.39
R_{TIM} [b] ($mm^2\ K\ W^{-1}$)	30.5	511
$R_{AfMG/In/Si}$ [c] ($mm^2\ K\ W^{-1}$)	5.1	42.5

[a] Thermal conductivity of A-fMGs calculated according to an equation of $k = \alpha_{A-fMGs}\rho_{A-fMGs}C_{p,A-fMGs}$

[b] Thermal resistance caused by A-fMGs, calculated by $R_{A-fMG} = \frac{T}{k}$

[c] Calculated according to an equation of $R_{TIM} = \frac{L}{k_{TIM}} = 2R_{A-fMG/In/Si} + \frac{T}{k}$